Viscoelastic Material Models for more accurate Polyethylene Wear Estimation

SSAGE

Gioacchino Alotta[1], Olga Barrera[2] and Elise C. Pegg[3]

Abstract

Wear debris from ultra-high molecular weight polyethylene (UHMWPE) components used for joint replacement prostheses can cause significant clinical complications, and it is essential to be able to predict implant wear accurately *in vitro* to prevent unsafe implant designs continuing to clinical trials. The established method to predict wear is simulator testing, but the significant equipment costs, experiment time and equipment availability can be prohibitive. It is possible to predict implant wear using finite element methods, though those reported in the literature simplify the material behaviour of polyethylene and typically use linear or elasto–plastic material models. Such models cannot represent the creep or viscoelastic material behaviour and may introduce significant error. However, the magnitude of this error and importance of this simplification has never been determined. This study compares the volume of predicted wear from a standard elasto–plastic model, to a fractional viscoelastic material model. Both models have been fitted to experimental data. Standard tensile tests in accordance with ISO 527-3 and tensile creep-recovery tests were performed to experimentally characterise both (a) the elasto–plastic parameters and (b) creep and relaxation behaviour of the ultra-high molecular weight polyethylene. Digital image correlation technique was used in order to measure the strain field. The comparison of the predicted wear with the two models was performed on an explicit finite element model of a mobile–bearing unicompartmental knee replacement, and wear predictions were then made using Archard's law. The fractional viscoelastic material model predicted almost ten times as much wear compared to the elasto–plastic material representation. Furthermore, the viscoelastic model predicted sub–surface stresses in the polyethylene which are observed clinically. This work quantifies for the first time the error introduced by use of a simplified material model in polyethylene wear predictions, and shows the importance of representing the viscoelastic behaviour of polyethylene for wear predictions.

Keywords

Polyethylene wear; material model; fractional viscoelasticity; unicompartmental knee arthroplasty; finite element analysis

Introduction

Wear of ultra–high molecular weight polyethylene (UHMWPE) components used for joint replacement prosthesis can cause significant clinical complications, such as: implant loosening, osteolysis, inflammatory responses and post–operative pain **?**. It is, therefore, essential to be able to predict implant wear as accurately as possible *in vitro*, to minimise the risk of unsafe implant designs continuing to clinical trials. The established method to predict the wear of an implant is with simulator testing. Wear simulator tests have been well characterised and validated against clinical data, and can predict implant wear to an acceptable degree of accuracy so is regularly used for validaton of new designs **?**. However, wear simulator tests require significant equipment costs, availability of equipment is limited, and the experiments take a long time **?**.

Numerical simulation provides an alternative method to predict wear. Maxian *et al.* were the first researchers to use discretisation **?** to predict linear wear from a finite element model of an UHMWPE hip replacement component **??**. Maxian's work was based on a study by Marshek and Chen **?** who proposed that by applying Archard's wear equation to discrete elements of the articulating surfaces,

non-uniform contact pressures and geometries could be taken into account. Maxian *et al.* applied Marshek's approach finite element models of an UHMWPE acetabular cup. The linear wear (δh) was calculated for each individual node on the articulating surface for each time increment (Δt_i) from the contact stress (σ), the sliding distance (S) and the wear factor (K_w) (Equation **??**). Using this equation, the total wear for one cycle of loading was calculated for each node. To account for geometrical changes resulting from the wear, at a chosen number of cycles, the node positions are displaced by the calculated linear wear. Most reported studies apply a constant wear factor, but it has been shown that the wear factor of metal on UHMWPE varies depending on the

[1] Engineering and Architecture Faculty, University of Enna "Kore", Enna, Italy.
[2] Nuffield Department of Orthopaedics, Rheumatology and Musculoskeletal Sciences, University of Oxford, Oxford, UK
[3] Department of Mechanical Engineering, University of Bath, Bath, UK

Corresponding author:
Olga Barrera, Nuffield Department of Orthopaedics, Rheumatology and Musculoskeletal Sciences, Botnar Research Centre Windmill Road, Oxford, OX3 7LD, UK.

Email: olga.barrera@ndorms.ox.ac.uk

contact stress. This limitation was addressed by Onişoru *et al.* ?, who derived an equation to represent the relationship between contact stress and the wear factor, and applied this to their wear calculations, and reported an improved accuracy. Lui *et al.* ?? used a similar approach but also took account of cross-shearing effects to predict wear, based on work by Kang *et al.* ?.

$$\delta h_{node} = K_w \sum_{i=1}^{n} \sigma_i S_i \Delta t_i \qquad (1)$$

The majority of reported numerical wear studies for UHMWPE use linear isotropic material models to represent the material behaviour (Table ??), which is a simplification of the behaviour of the material. The first study to calculate wear using a more complex material model for polyethylene was Teoh *et al.* ?, who used a bilinear elastoplastic material representation. The authors reported a significant increase in contact stresses and wear with the elastoplastic model. Although an improvement, elastoplastic material models cannot represent material behaviour such as creep, stress–relaxation, kinematic hardening or rate–dependence, all of wihch are observed with polyethylene. Bevill *et al.* ? included creep behaviour in their wear calculations which enabled them to distinguish between linear wear and creep deformation giving valuable insight into the clinical scenario, and Lui *et al.* ?? used a similar approach. However, neither study directly compared the difference the use of a more representative material model for UHMWPE had on the predicted wear rate.

Table 1. Ultra-high molecular weight polyethylene material representation and wear calculations used in finite element wear analyses reported in the literature, where K is the Wear Factor

Author Year	Material model	K (mm³N⁻¹mm⁻¹)
Maxian ?? 1996	Linear elastic	1.06×10^{-9}
Brown ? 2002	Linear elastic	1.06×10^{-9}
Teoh ? 2002	Elastoplastic	1.06×10^{-9}
Wu ? 2003	Linear elastic	0.8×10^{-9}
Bevill ? 2005	Creep	1.06×10^{-9}
Onişoru ? 2006	Linear elastic	$7.99\sigma^{-0.653} \times 10^{-9}$
Fialho ? 2007	Linear elastic	1.06×10^{-9}
Pal ? 2008	Elastoplastic	2.64×10^{-13}
Kang ? 2009	Linear elastic	1.24×10^{-9}
Lui ? 2012	Creep	n/a
Innocenti ? 2014	Linear elastic	1.83×10^{-14}
Netter ? 2015	Linear elastic	0.17×10^{-9}

Viscoelastic material behaviour (creep, stress–relaxation, as well as a "fading" memory effect) can be represented by a combination of elastic behaviour (springs) and viscous behaviour (dashpots). The Maxwell or Kelvin–Voigt models are examples of spring and dashpot models; these have the advantage of fast impementation and can describe time–dependent behaviour but cannot accurately represent polyethylene. Increasing complexity, with multiple springs and dashpots in different arrangements (such as Zener models) can capture the creep and relaxation behaviour but are computationally very demanding. An alternative approach is the use of fractional viscoelastic material models, which have been used successfully to represent very complex

material properties for both short and long term time behaviour. A three dimensional fractional viscoelasticity theory has been derived and discussed in ?. Furthermore, the implementation in commercial FE software of a range of fractional viscoelastic models including fractional Maxwell, Kelvin- Voigt and Zener among others has been presented in ?. The purpose of the present study was to investigate whether the application of a viscoelastic material model to represent UHMWPE alters the predicted wear from a finite element model. A fractional viscoelastic material model was fit to experimentally derived data (which have not been presented elsewhere), and then applied to a finite element model of a mobile unicompartmental knee replacement (The Oxford Knee, Zimmer-Biomet) to examine the influence on wear. We report differences in the predicted wear for a simple ramp–loading scenario as a preliminary study, with a view to increasing the model complexity as future work.

Materials and Methods

Development of the fractional viscoelastic material model

In classical viscoelasticity the constitutive behaviour is obtained by combining the feature of springs (elastic elements) and dashpots (viscous elements). The mechanical models obtained with this approach are characterized by exponential relaxation and creep function. However, it was first observed at the beginning of the twentieth century that creep and relaxation test of many polymers is well fitted by power law functions ? (with power lying in the range $0 \div 1$). In the frame of linear viscoelasticity, the Boltzmann superposition principle ? it is assumed to be valid. If power law creep/relaxation functions of the type

$$R(t) = \frac{C_{\bar{\alpha}} t^{-\bar{\alpha}}}{\Gamma(1 - \bar{\alpha})} \qquad (2a)$$

$$C(t) = \frac{t^{\bar{\alpha}}}{C_{\bar{\alpha}} \Gamma(1 + \bar{\alpha})} \qquad (2b)$$

are assumed, the Boltzmann superposition principle leads directly to constitutive law involving the so called fractional operators. These are neither else than integro-differential operators of real order defined as convolution integrals with power law kernel ?; in viscoelasticity the order of integrals/derivatives is in the range $0 \div 1$. In Eqs. (??) $R(t)$ and $C(t)$ denote the creep and relaxation function, respectively, $C_{\bar{\alpha}}$ and $\bar{\alpha}$ are parameters, with $0 \le \bar{\alpha} \le 1$ and correspondent with order of derivative (or integral), and $\Gamma(\cdot)$ is the Euler gamma function.

The most simple model is the *springpot*, often represented as a rhombus (see Fig. ??). The constitutive equation of this model can be written as ??

$$\sigma(t) = C_{\bar{\alpha}} \left({}^{C}D^{\bar{\alpha}}\varepsilon \right)(t) \qquad (3a)$$

$$\varepsilon(t) = \frac{1}{C_{\bar{\alpha}}} \left(I^{\bar{\alpha}}\sigma \right)(t) \qquad (3b)$$

where $\left({}^{C}D^{\bar{\alpha}} \cdot \right)$ and $\left(I^{\bar{\alpha}}\sigma \right)$ are the Caputo's fractional derivative and the Riemann-Liouville fractional integral ?, respectively. For the simplicity of the notation, in the
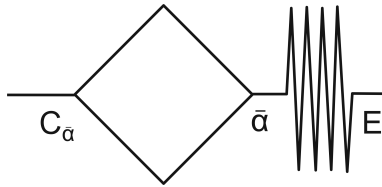
Figure 1. Schematic illustration of the fractional Maxwell model

following the Caputo's fractional derivative will be denoted simply by $(D^{\bar{\alpha}} \cdot)$

The main advantages of the springpot model are that it is able to reproduce the power law behaviour observed experimentally and that it has long fading memory in agreement with the real behaviour of many materials. Moreover, it has been demonstrated that the behaviour of the springpot can be reproduced in classical viscoelasticity only by means of infinite sequence of springs and dashpots **??**.

It is to be noted that in Eq. (**??**) $R(0) = \infty$ and $R(\infty) = 0$, $C(0) = 0$ and $C(\infty) = \infty$. However, experimental tests with many viscoelastic materials have revealed that often the relaxation and creep functions exhibit an initial ($t = 0$) and/or a long term ($t \to \infty$) finite value. For this reason the springpot model is often used in combination with one or more springs. Experimental tests on UHMWPE considered in this work are well reproduce by a springpot in series with a spring, namely a Fractional Maxwell model (depicted in Fig. **??**). This result has been obtained by the authors in the experimental campaign described in the next section and is also confirmed by previous works **?**. The constitutive law of the Fractional Maxwell model is written as follows.

$$(D^{\bar{\alpha}}\sigma)(t) + \frac{E}{C_{\bar{\alpha}}}\sigma(t) = E(D^{\bar{\alpha}}\epsilon)(t) \qquad (4)$$

where E is the Young modulus related to the spring. The relaxation and creep functions of the fractional Maxwell model can be easily obtained as:

$$R(t) = E E_{\bar{\alpha}}\left(-\frac{E}{C_{\bar{\alpha}}}t^{\bar{\alpha}}\right) \qquad (5a)$$

$$C(t) = \frac{1}{E} + \frac{t^{\bar{\alpha}}}{C_{\bar{\alpha}}\Gamma(1+\bar{\alpha})} \qquad (5b)$$

being $E_{\bar{\alpha}}(\cdot)$ the one parameter Mittag-Leffler function defined as [citare Podlubny]

$$E_{\bar{\alpha}}(z) = \sum_{k=0}^{\infty} \frac{z^k}{\Gamma(1+\bar{\alpha}k)} \qquad (6)$$

Eqs. (**??**) and (**??**) are related to an unidimensional model; indeed, Eq. (**??**) has been assumed as a basis for the fitting of the experimental test described in the next section. However, for the finite element analysis a three dimensional model has to be defined. Assuming that the material is isotropic, only two relaxation or creep function are needed in order to characterize the three dimensional behaviour of the material, one describing the pure volumetric behaviour and the other one describing the pure shear behaviour **???**. In compact form the terms of the relaxation matrix are written:

$$R_{ijkh}(t) = \left(K_R(t) - \frac{2}{3}G_R(t)\right)\delta_{ij}\delta_{kh} \\ + G_R(t)\left(\delta_{ik}\delta_{jh} + \delta_{ih}\delta_{jk}\right) \qquad (7)$$
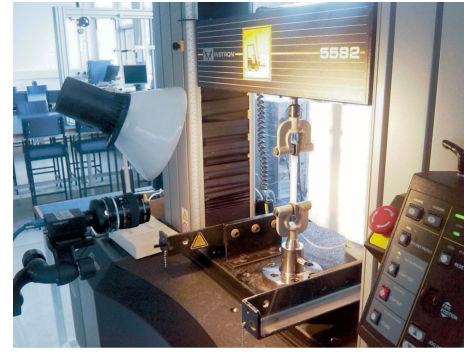

Figure 2. Experimental equipment used for the viscoelastic characterisation of the UHMWPE material

where $K_R(t)$ and $G_R(t)$ are the relaxation functions of the pure volumetric and pure shear components, respectively, and δ is the Kronecker delta. Assuming that both the components are well reproduced by Fractional Maxwell models, the relaxation and creep functions are analogous to Eqs. (**??**). The function related to the volumetric contribution are obtained from Eqs. (**??**) by substituting E, $C_{\bar{\alpha}}$ and $\bar{\alpha}$ with K, K_β and β, respectively. The function of the shear contributions are obtained from Eqs. (**??**) by substituting E, $C_{\bar{\alpha}}$ and $\bar{\alpha}$ with G, G_α and α, respectively.

In agreement with experimental evidence, the volumetric and shear time scales, which are determined by the parameters α and β, are not assumed equal **???**. This allow the model to be very flexible and to reproduce also time varying Poisson's ratio **?**.

Experimental determination of UHMWPE viscoelastic parameters

Uniaxial Creep–recovery experimental tests were performed to characterize the parameters to use for the viscoelastic material model. Tensile test specimens were machined from in–house sheet moulded UHMWPE, made from GUR 4150 resin (Celanese, Germany), which is the non–medical grade equivalent of GUR 1050. The samples were machined to a rectangular geometry of 180 mm by 20 mm by 1 mm. The strain in the direction of the applied stress was measured by means of the Digital Image Correlation technique.

Tensile tests were performed on an electromechanical test machine (5582, Instron) (Figure **??**).

Different magnitude of the constant applied stress σ_0 load have been applied: 1, 3 and 5 MPa (see Figure **??**). The parameters obtained by the fitting of experimental data at different level of stress are homogeneous. For this reason the material can be considered linearly viscoelastic at the least up to 5 MPa of applied stress. This fact is confirmed by results published in **?** where it is shown that UHMWPE may be considered linear up to 10 MPa.

The maximum tensile stress σ_0 was reached after 4 minutes of ramp loading. The stress was maintained for 6 hours, after which the load was reduced to zero over a period of 4 minutes, and the samples were left to recover for 6 hours (see Figure **??**).

The fitting of experimental data has taken into account the exact history of stress describe above and to this purpose it is

written as:

$$\sigma(t) = \frac{\sigma_0}{t_0} \{ [t - (t - t_0)U(t - t_0)] \\ - [(t - t_1)U(t - t_1) - (t - t_2)U(t - t_2)]\} \tag{8}$$

where $t_0 = 4$ minutes is the time at the end of the loading ramp, $t_1 = 364$ minutes is the time at the end of the creep phase, $t_2 = 368$ minutes is the time at the end of the unloading ramp and $U(t)$ is the unit-step function. By assuming the creep function of Eq. (**??**), the history of stress of Eq. (**??**) generates the following theoretical history of strain (see Figure **??**) that was used to fit experimental test:

$$\epsilon(t) = \frac{\sigma_0}{Et_0} \{ [t - (t - t_0)U(t - t_0)] \\ - [(t - t_1)U(t - t_1) - (t - t_2)U(t - t_2)]\} \\ + \frac{\sigma_0}{C_{\bar{\alpha}}t_0} \{ [t^{1+\bar{\alpha}} - (t - t_0)^{1+\bar{\alpha}}U(t - t_0)] \\ - [(t - t_1)^{1+\bar{\alpha}}U(t - t_1) - (t - t_2)^{1+\bar{\alpha}}U(t - t_2)]\} \tag{9}$$

The values of the obtained parameters E, $C_{\bar{\alpha}}$ and $\bar{\alpha}$ are reported in Table 3. The parameters related to the three dimensional constitutive law (G, G_α, α, K, K_β and β) are reported in Table 4. These have been obtained by considering a constant Poisson's ratio $\nu = 0.46$ (value commonly considered for UHMWPE) and the following well known relationships has been used:

$$G = \frac{E}{2(1 + \nu)} \tag{10a}$$

$$K = \frac{E}{3(1 - 2\nu)} \tag{10b}$$

Analogous relationships have been used to obtain G_α and K_β from $C_{\bar{\alpha}}$. The hypothesis of constant Poisson's ratio implies also that $\alpha = \beta = \bar{\alpha}$; this means that the volumetric and shear contribution evolve with the same time scale. This fact is in disagreement with experimental results **??**. However, the direct determination of the two time scales may be performed only if in the uniaxial creep test we are able to measures correctly not only the longitudinal strain but also the transverse strain. Another strategy is to perform two different creep test, as an example the uniaxial creep test and a torsion creep test. In this work it has not been possible to perform a double measure in the uniaxial creep test. Moreover, for the scope of the work, that is to compare the predicted wear with a commonly used elasto-plastic model and with a fractional viscoelastic model, this approximation is acceptable. Of course, a more precise characterization of the three dimensional constitutive behaviour is desirable in order to predict with less approximation the response of the UHMWPE bearing and the wear of its surface.

Finite element model definition

The finite element model consisted of an UHMWPE unicompartmental knee bearing component (The Oxford Partial Knee, Zimmer-Biomet), and an articulating femoral component modelled as an analytical rigid body. Drawings of both component geometries has been previously published **?**. The femoral component was a sphere of radius 24 mm,
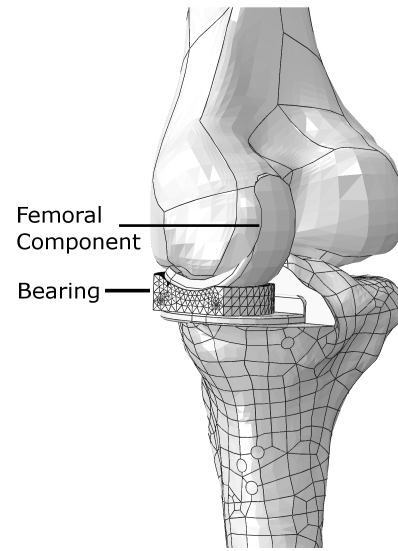

Figure 3. Illustration of the finite element model assembly, where the meshed bearing and articulating femoral components are shown in the context of the knee. The femur, tibia and tibial component did not contribute to the model, but are included for illustrative purposes.

cut to a width of 20 mm. The upper articulating surface of the bearing conformed to the femoral component with a clearance of 0.2 mm. The thickness of the bearing in the centre was 3.5 mm, and the bearing was 34 mm long by 24 mm wide. Holes for marker wires were included and positioned 3 mm from the base of the bearing, and the marker wires themselves were represented as rigid cylinders of 1 mm diameter.

The components were assembled as is shown in Figure **??**; the femur, tibia, and tibial component did not contribute to the model but are included for illustrative purposes. The load was applied axially to the femoral component, perpendicular to the base of the bearing. The component was compressively ramp loaded to 1200 N over a period of 0.2 s. The base of the bearing was constrained in the axial direction. Contact was defined between the femoral component and the upper surface of the bearing, with penalty friction of 0.08 **?**. Tie constraints were used to fix the marker wires within the bearing. The bearing was meshed with quadratic tetrahedral element (C3D10M), and the converged mesh size was used, the determination of which is described in Section **??**.

The material properties defined to the metallic components was limited to the density, as these were modelled as rigid bodies. The femoral component was modelled with a density of 8.387 g cm^{-3} to represent Cobalt-Chromium-Molybdenum alloy **?**, and the marker wires were assigned a density of 4.42 g cm^{-3} for Titanium-6-Aluminium-4-Vanadium alloy **?**. A subroutine was created to apply the fractional viscoelastic model described in Section **??**. For the elasto-plastic material model a modulus of 855.2 MPa was used, a Poisson's ratio of 0.46, and the plasticity parameters are summarised in Table **??**. These values were determined after testing the sheet moulded GUR 4150 in accordance with ISO 527-3 using Specimen Type 2 geometry.

Table 2. Plastic material properties defined for the elasto-plastic models

True stress (MPa)	True plastic strain
2.8	0.00
9.2	0.01
13.5	0.02
16.4	0.03
18.3	0.04
21.7	0.07

All models were created, solved, and post-processed using Abaqus finite element software (version 6.12, Dassault Systémes, Paris, France). An explicit solver was used with an imposed time increment of 4×10^{-6}.

Quantification of wear

Linear wear was calculated for the two different models using Equation **??**. A wear factor of 1.06×10^{-9} mm^3 N^{-1} mm^{-1} was used, as reported by Maxian *et al.* **??**. The linear wear for each time increment was the maximum linear wear of all the nodes on the articulating surface. The volumetric wear was the sum of the linear wear of all the nodes on the articulating surface multiplied by the surface area (766.2 mm^2).

The sliding distance (S) was calculated using the great-circle distance equation (Equation **??**), which assumed the sliding occurred around the circumference of the femoral component. The cartesian co-ordinates of the position of the nodes at the start and the end of the increment were converted to polar co-ordinates (ϕ_1, λ_1 and ϕ_2, λ_2, respectively) relative to the centre of the femoral component, and the femoral component radius (24 mm) was used as the sphere radius (R).

$$S = 2.R.sin^{-1}\left[sin^2\left(\frac{\phi_2 - \phi_1}{2}\right) + cos(\phi_1).cos(\phi_2).sin^2\left(\frac{\lambda_2 - \lambda_1}{2}\right)\right]^{0.5} \quad (11)$$

Mesh convergence

The mesh convergence was performed for the linear wear and volumetric wear output. The mesh seeding densities examined were from 2.0 mm to 5.0 mm with 0.5 mm intervals, which created between 115 and 526 nodes on the articular surface. Both the linear wear and gravimetric result converged at a mesh size of 3.5 mm (Figure **??**).

Results

Definition of the fractional viscoelastic material model

The results of the creep–recovery experimental tests were fitted to the fractional viscoelastic Maxwell model as shown in Figure **??**. The fitted parameters are summarised in Table **??**. It can be seen that the parameters were of a good fit to the experimental data. These data were then converted into the parameters necessary for the fractional viscoelastic model as described in the previous section, and these are summarised in Table **??**.
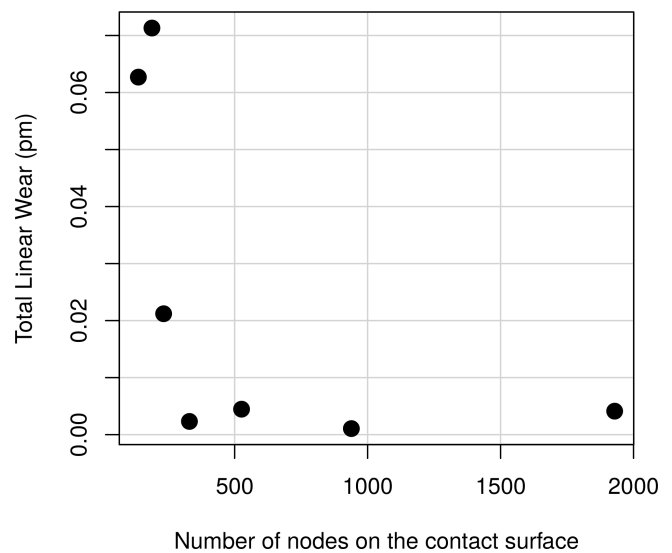
Figure 4. Variation of the calculated linear wear for different numbers of nodes on the contact surface. A mesh size of 3.5 mm was deemed convergenced (189 nodes).
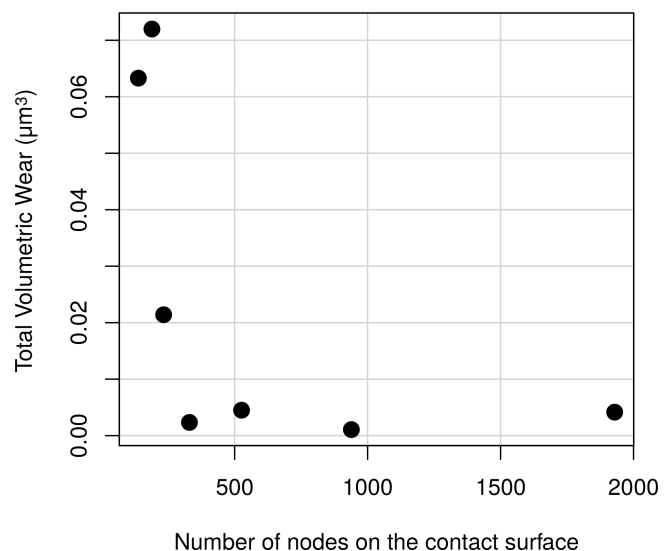
Figure 5. Variation of the calculated volumetric wear for different numbers of nodes on the contact surface. A mesh size of 3.5 mm was deemed convergenced (189 nodes).

Table 3. Parameters determined from the creep–recovery test results to represent GUR 4150 UHMWPE

Parameter	Value
$\bar{\alpha}$	0.4
$C_{\bar{\alpha}}$	24553 M Pas$^{\bar{\alpha}}$
E	561 MPa

Table 4. Input parameters for the fractional Maxwell model, identified from the creep-recover test results

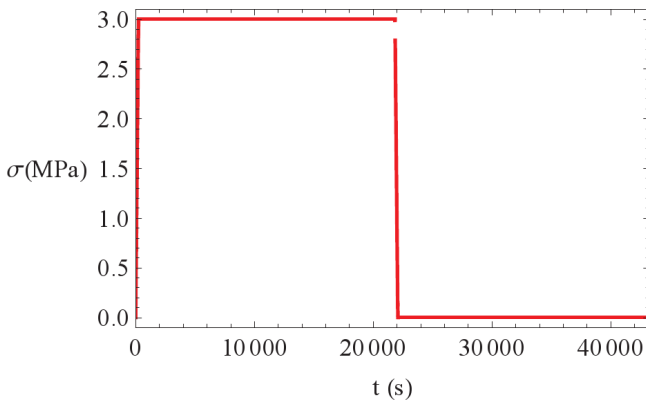| Parameter	Value
K	2338 MPa
G	192 MPa
K_{β}	102304 M Pa s$^{\beta}$
G_{α}	8404 M Pa s$^{\alpha}$
α	0.4
β	0.4

Figure 6. Variation of stress with time during the creep recovery test. Test results are shown in red, and the theoretical curve with the fitted parameters is shown in black
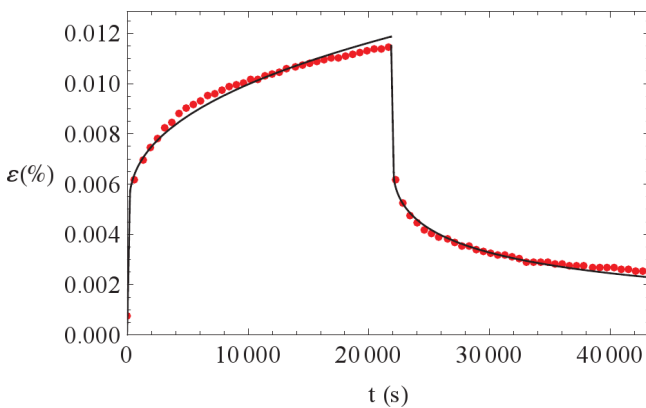

Figure 7. Variation of strain with time during the creep recovery test. Test results are shown in red, and the theoretical curve with the fitted parameters is shown in black

Wear volume prediction

The wear prediction (for both linear and volumetric wear) using the fractional viscoelastic material model to represent UHMWPE was almost 10 times greater than that predicted using an elasto-plastic material model (Figure **??**). When the wear factor was calculated using the Onişoru equation **?**, this difference was even greater but the overall predicted wear was reduced.

The cumulative increase in wear (both linear and volumetric) was approximately linear for the elasto–plastic material model (coefficient of determination = 0.912 for linear wear, and 0.834 for volumetric wear). Whereas the viscoelastic model deviated from linearily at higher loads(Figure **??**).

Stress analysis

The overall stress within the bearing was increased when the UHMWPE was represented as a viscoelastic material, but in particular a difference was noticed in the stress on the contact surface and in the contact region. Figure **??** illustrates a cross-section through the centre of the bearing for the two different material models. It can be seen that in the viscoelastic model the stress is more concentrated around the articulating surface, whereas in the elastoplastic material model the stress is evenly distributed through the thickness of the bearing.
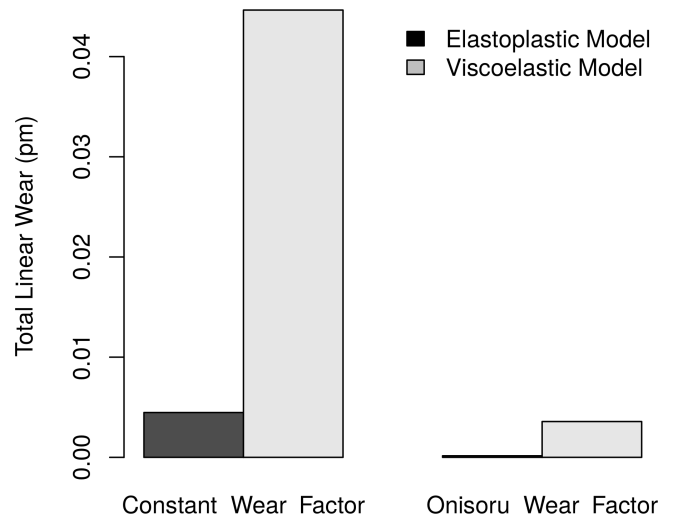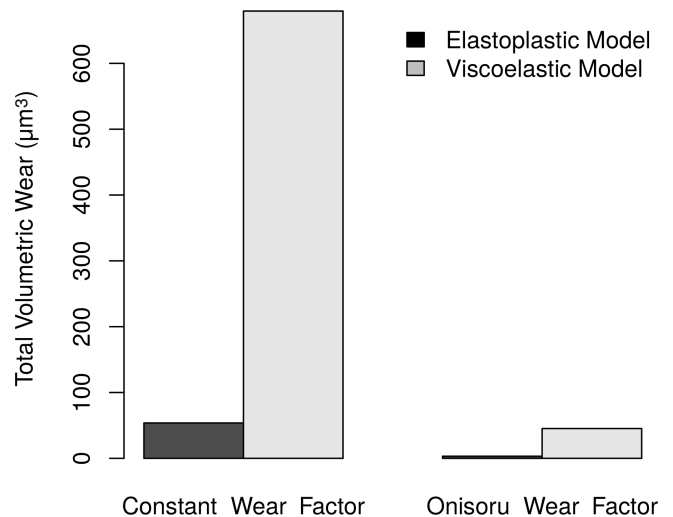

Figure 8. Calculated total linear wear for the elastoplastic material model and the fractionalelastic material model. Results using a constant wear factor of 1.06×10^{-9} mm^3 N^{-1} mm^{-1}, and the Onisoru wear factor which used a variable wear factor calculated from the contact stress ($7.99\sigma^{-0.653}$)

Figure 9. Calculated total volumetric wear for the elastoplastic material model and the fractionalelastic material model. Results using a constant wear factor of 1.06×10^{-9} mm^3 N^{-1} mm^{-1}, and the Onisoru wear factor which used a variable wear factor calculated from the contact stress ($7.99\sigma^{-0.653}$)

Discussion

The results of this study have demonstrated a clear difference in the wear prediction from a finite element model of an UHMWPE component when using a viscoelastic material model definition compared with an elastoplastic model. It is known that elasto–plastic material models will underestimate stress due to the stress-relieving effect of plasticity. However, numerous authors have used linear elastic material models to predict wear and the results have correlated well with with either experimental wear test data, or clinical data. It is therefore unexpected that a more representative material model can have such a large influence on the predicted wear.

One possible reason for this discrepancy could be the wear factor. As shown in Table **??**, a wide range of wear coefficients are reported in the literature; values range from 0.00002 x 10^{-9} mm^3 N^{-1} mm^{-1} to 1.2 x 10^{-9} mm^3 N^{-1}
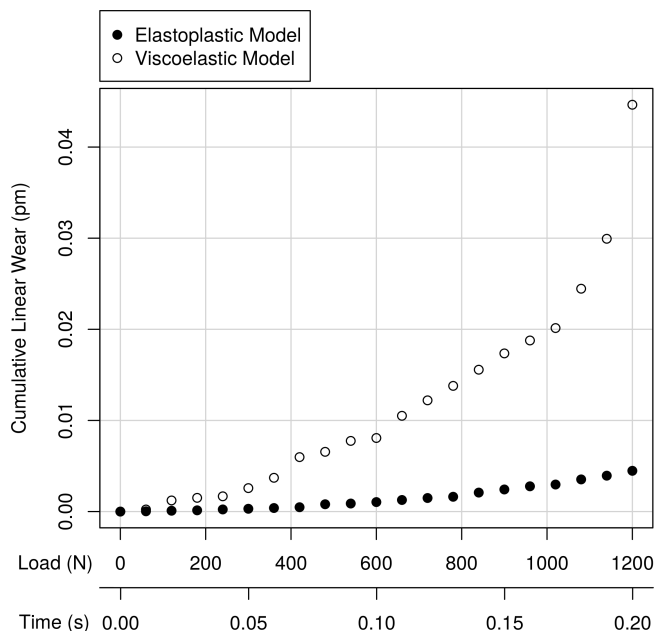
Figure 10. Cumulative linear wear during the loading step. Results are shown for the Elastoplastic material model, and the fractional viscoelastic material model, calculated using a constant wear factor of 1.06 x10^{-9} mm^3 N^{-1} mm^{-1}.
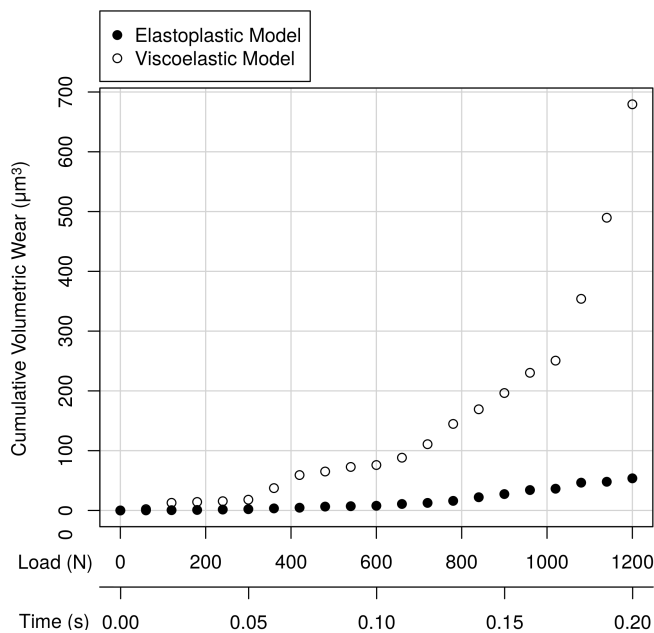

Figure 11. Cumulative volumetric wear during the loading step. Results are shown for the Elastoplastic material model, and the fractional viscoelastic material model, calculated using a constant wear factor of 1.06 x10^{-9} mm^3 N^{-1} mm^{-1}.
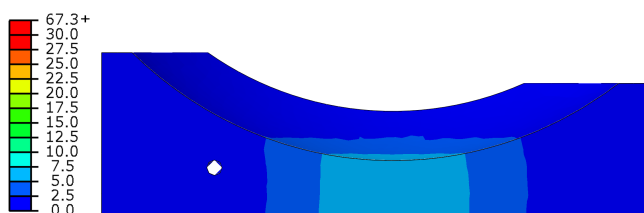

Figure 12. Cross–sectional view through centre of the unicompartmental knee bearing in the sagittal plane. The von Mises stress distribution within the bearing is illustrated for the results using the elastoplastic material model
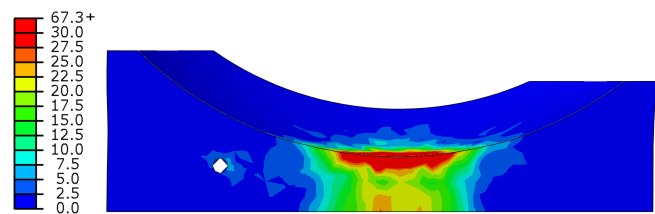

Figure 13. Cross–sectional view through centre of the unicompartmental knee bearing in the sagittal plane. The von Mises stress distribution within the bearing is illustrated for the results using the fractional viscoelastic model

mm^{-1}. The majority of wear factors are calculated from pin–on–disk experiments which can have a simplified loading scenario compared to *in vivo* loading, but some studies have used simulator wear results, and clinically derived data to calculate wear factors **?** which are likely to be more representative. Nevertheless, there is a need for more research to accurately determine the wear factor of metal on UHMWPE for different situations to ensure the accuracy of numerical wear predictions.

Despite being a more accurate representation of the material behaviour, it may be that the increased wear predicted by the viscoelastic model is not representative of reality. UHMWPE is known to harden due to alignment of molecular chains under cyclic loading, and also due to oxidation over time *in vivo*. Neither the viscoelastic model, nor the elastoplastic model, takes into account the hardening. Including hardening effects into the model would reduce the wear rate. It could be that inclusion of kinematic hardening into the material model, or alteration of the wear factor with loading cycles could create a more realistic prediction of wear. Use of the wear factor to represent so called "running in wear" was reported by Liu *et al.* **?**, who examined wear of metal–on–metal hip replacements using finite element analysis. The wear was calculated by defining two wear coefficients, one for short–term wear, and one for long–term wear. It may be possible to use a similar methodology to represent hardening and sub-surface oxidation of UHMWPE with time while maintaining computational efficiency.

Another factor to consider in the wear calculation is determination of the sliding distance. In the present study the sliding distance was calculated using the great–circle distance equation, which was possible due to the conforming nature of the articulating surfaces and the spherical geometry. In the design of the Oxford Unicompartmental Knee there is a 0.2 mm clearance between the femoral component and the bearing. In the present study, because the femoral component was modelled as a rigid part, it was valid to assume that where contact occurred on the bearing surface, that this clearance must have been closed by deformation of the bearing. However, if material properties had been assigned to the femoral component use of the great–circle distance equation could have introduced errors. Studies in the literature often do not mention how sliding distance has been calculated. Teoh *et al* mention using the great–circle distance equation to calculate the sliding distance. Other studies calculate the sliding distance based upon a defined rotational or translational displacement **?**, but these assume no change in the component geometry. However, the

influence of this assumption would be expected to be minor in the case of large displacements and small wear.

Conclusions

In conclusion, this study has shown the use of simplified material models to represent polyethylene to predict wear introduces significant (up to 10 times) error in the calculated wear volume. In contrast, the fractional viscoelastic material model, which was defined from experimental data, predicted concentrated stresses on the articulating surface, which is matches well with sub–surfaces stresses reported from retrieved components **?**. Use of such accurate material models in finite element models of joint replacements could prove to be a cost-efficient, reliable way to predict wear and aid optimal implant design.

Acknowledgments

Author Contributions

O.B. and E.P designed the study. G.A. and O.B. performed the mechanical testing and created the fractional viscoelastic material model. E.P. developed the finite element model and G.A. implemented the fractional viscoelastic material code. E.P performed the data analysis and wrote the paper and O.B. and G.A. edited the manuscript.

Conflict of interests

The authors declare no conflict of interest.

References

Goodman, S.B. Wear particles, periprosthetic osteolysis and the immune system. *Biomaterials* **2007**, *28*, 5044-5048.

Essner, A.; Schmidig, G.; Wang, A. The clinical relevance of hip joint simulator testing: In vitro and in vivo comparisons. *Wear* **2005**, *259*, 882-886.

Netter, J.; Hermida, J.; Flores–Hernandez, C.; Steklov, N.; Kester, M.; D'Lima, D.D. Prediction of Wear in Crosslinked Polyethylene Unicompartmental Knee Arthroplasty. *Lubricants* **2015**, *3*, 381-393.

Marshek, F.M; Chen, H.H. Discretization pressure–wear theory for bodies in sliding contact. *J Tribol* **1989**, *111*, 95-101.

Maxian, T. A.; Brown, T. D.; Pedersen, D. R.; Callaghan, J.J. A sliding–distasnce–coupled finite element formulation for polyethylene wear in total hip arthroplasty. *J Biomech* **1996**, *29*, 687-692.

Maxian, T. A.; Brown, T. D.; Pedersen, D. R.; Callaghan, J.J. Adaptive finite element modeling of long–term polyethylene wear in total hip arthroplasty. *J Orthop Res* **1996**, *14*, 668-675.

Innocenti, B.; Labey, L.; Kamali, A.; Pascle, W.; Pianigiani, S. Development and Validation of a Wear Model to Predict Polyethylene Wear in Total Knee Arthroplasty: A Finite Element Analysis. *Lubricants* **2014**, *2*, 193-205.

Onişoru, J.; Capitanu, L.; Iarovici, A. Prediction of wear of acetabulum inserts due to multiple human routine activities *Tribology* **2006**, *8*, 28-33.

Lui, F.; Fisher, J.; Jin, Z. Computational modelling of polyethylene wear and creep in total hip joint replacements: Effect of the bearing clearance and diameter. *Proc IMechE Part J* **2012**, *226*, 551-563.

Lui, F.; Fisher, J.; Jin, Z. Effect of motion inputs on the wear prediction of artifial hip joints. *Tribology Int* **2013**, *63*, 105-114.

Kang, L.; Galvin, A.L.; Brown, T.D.; Jin, Z.; Fisher, J. Quantification of the effect of cross-shear on the wear of conventional and highly cross-linked UHMWPE *J Biomechanics* **2008**, *41*, 340-346.

Teoh, S.H.; Chan, W. H.; Thampuran, R. An elasto–plastic finite element model for polyethylene wear in total hip arthroplasty. *J Biomech* **2002**, *35*, 323-330.

Bevill, S. L.; Bevill, G. R.; Penmetsa, J. R.; Petrella, A. J.; Rulkoetter, P. J. Finite element simulation of early creep and wear in total hip arthroplasty. *J Biomech* **2005**, *38*, 2365-2374.

Brown, T.D.; Steward, K.J.; Nieman, J.C.; Pedersen, D.R.; Callaghan, J.J. Local head roughening as a factor contributing to variability of total hip wear: a finite element analysis *J Biomech Eng* **2002**, *124*, 691-698.

Wu, J.S-S; Hung, J-P.; Shu, C-S.; Chen, J-H. The computer simulation of wear behaviour appearing in total hip prosthesis *Comput Meth Prog Bio* **2003**, *70*, 81-91.

Fialho, J.C.; Fermandes, P.R.; Eça, L; Folgado, J. Computational hip joint simulator for wear and head generation. *J Biomech* **2007**, *40*, 2358-2366.

Pal, S.; Haider, H.; Laz, P. J.; Knight, L. A.; Rulkoetter, P. J. Probabilistic computational modeling of total knee replacement wear *Wear* **2008**, *264*, 701-707.

Kang, L.; Galvin, A.L.; Fisher, J.; Jin, Z. Enhanced computational prediction of polyethylene wear in hip joints by incorporating cross–shear and contact pressure in additional to load and sliding distance: Effect of head diameter. *J Biomech* **2009**, *42*, 912-918.

Wang, A. A unified theory of wear for ultra–high molecular weight polyethylehe in multi–directional sliding. *Wear* **2001**, *248*, 38-47.

Liau, J-J.; Cheng, C-K.; Huang, C-H.; Lo, W-H. The effect of malalignment on stresses in polyethylene component of total knee prostheses - a finite element analysis. *Clin Biomech* **2002**, *17*, 140-146.

Patil, S.; Bergula, A.; Chen, P. C.; Colwell, C. W.; D'Lima, D.D. Polyethylene wear and acetabular component orientation. *J Bone J Surg* **2003**, *85*, 56-63.

Pegg, E.C.; Murray, D.W.; Pandit, H.G.; O'Connor, J.J.; Gill, H.S. Fractureo f mobile unicompartmental knee bearings: A parametric finite element study. *Proc ImechE Part H* **2013**, *227*, 1213-1223.

El-Domiaty, A.; El-Fadaly,M.; Es Nassef, A. Wear characteristics of ultrahigh molecular weight polyethylene (UHMWPE). *J Mat Eng Perf* **2002**, *11*, 577-583.

Georgette, F.S. Effect of hot isotatic pressing on the mechanical and corrosion properties of a case, porous-coated Co-Cr-Mo alloy. In *Quantitative Characterization and Performance of Porous Implants for Hard Tissue Applications*; ASTM International: Philadelphia, P.A, 1987; pp. 16.

Harrysson, O.L.A.; Cansizoglu, O.; Marcellin–Little, D.J.; Cormier, D.R.; Wear, H.A. Direct metal fabrication of titanium implants with tailored materials and mechanical properties using electron beam melting technology. *Mat Sci Eng* **2008**, *28*, 366-373.

Liu, F.; Jin, Z. Roberts, P.; Grigoris, P. Importance of head diameter, clearance, and cup wall thickness in elastohydrodynamic lubrication analysis of metal-on-metal hip resurfacing prostheses. *Proc Inst Mech eng H* **2006**, *220*, 695-704.

Landy, M.M.; Walker, P.S. Wear of ultra-high-molecular-weight polyethylene components of 90 retrieved knee prostheses *J Arthop* **1988**, *3*, S73-S85.

Nutting, P.G. A new general law of deformation *J Frankl Inst* **1921**, *191*, 679-685.

Christensen, R.M. Theory of viscoelasticity. An introduction *Academic Press, New York* **1982**.

Podlubny, I. Fractional differential equation *Academic Press, San Diego* **1999**.

Gemant, A. A Method of Analyzing Experimental Results Obtained from Elasto-Viscous Bodies *Physics* **1936**, *7*, 311-317.

Scott-Blair, G.W.; Caffyn J.E. An application of the theory of quasi-properties to the treatment of anomalous strain-stress relations *Philos Mag* **1949**, *40*, 80-94.

Schiessel, H.; Blumen, A. (1993) Hierarchical Analogues to Fractional Relaxation Equations. *J Phys A: Math General* **1993**, 26: 5057-5069.

Di Paola, M.; Pinnola, F.P.; Zingales, M. (2013) A discrete mechanical model of fractional hereditary materials *Meccanica* **48**,1573-1586.

Guedes, R.M. A viscoelastic model for a biomedical ultra-high molecular weight polyethylene using the time-temperature superposition principle *Polym Test* **2011**, *30*, 294-302.

Makris N. Three-dimensional constitutive viscoelastic laws with fractional order time derivatives *J Rheology* **1997**, *41*, 1007-1020.

Freed, A.D.; Diethelm, K. Fractional calculus in biomechanics: a 3D viscoelastic model using regularized fractional derivative kernels with application to the human calcaneal fat pad *J Biomech Sci Eng* **2006**, *5*, 203-215.

Alotta, G.; Barrera, O.; Cocks, A.C.F.; Di Paola, M. On the behavior of a three-dimensional fractional viscoelastic constitutive model *Meccanica* **2016**, 1-16.

Alotta, G.; Barrera, O.; Cocks, A.C.F.; Di Paola, M. The finite element implementation of 3D fractional viscoelastic constitutive models Submitted to *Finite element analysis and design* **2017**

Lakes, R.S. The time-dependent Poisson's ratio of viscoelastic materials can increase or decrease *Cellular Polymers* **1992**, *11*, 466-469.

Mourad, A.-H.I.; Fouad, H.; Elleithy, R. Impact of some environmental conditions on the tensile, creep-recovery, relaxation, melting and crystallinity behaviour of UHMWPE-GUR 410-medical grade *Materials and Design* **2009**, *30*, 4112-4119.